Phosphatase PP2A is essential for TH17 differentiation

Phosphatase PP2A is essential for T_H17 differentiation

Short title: PP2A is essential for T_H17 differentiation

Qin Xu[1,2], Xuexiao Jin[1,2,3], Mingzhu Zheng[1,2], Deepak Rohila[1,2], Guotong Fu[1,2], Zhuoyu Wen[1,2], Jun Lou[1,2], Songquan Wu[4], Richard Sloan[5], Lie Wang[6], Hu Hu[7], Xiang Gao[8,*], Linrong Lu[1,2,3,9,10,*]

[1]Institute of Immunology, and Department of Dermatology and Rheumatology in Sir Run Run Shaw Hospital, [2]Program in Molecular and Cellular Biology, [3]ZJU-UoE Institute, [6]Department of Immunology, [7]Pathology and Pathophysiology, [9]Innovation Center for Cell Signaling Technology Network, [10]Dr. Li Dak Sum & Yip Yio Chin Center for Stem Cell and Regenerative Medicine, Zhejiang University School of Medicine, Hangzhou 310058, P. R. China.

[4]Medical College of Lishui University, Lishui, Zhejiang 323000, China

[5]Division of Infection and Pathway Medicine, The University of Edinburgh, Edinburgh EH16 4SB, Scotland, UK

[8]Key Laboratory of Model Animals for Disease Study of the Ministry of Education, Model Animal Research Center, Nanjing University, Nanjing 210061, P. R. China.

These authors contributed equally to this work: Qin Xu and Xuexiao Jin.

*Correspondence authors: L.L. (email: lu_linrong@zju.edu.cn) and X.G. (email: gaoxiang@nju.edu.cn)

Lead Contact: Linrong Lu, 866 Yuhang Tang Road, Medical Research Building A807, Hangzhou, 310058, P. R. China. Tel: 86-571-88981173; Email: lu_linrong@zju.edu.cn.

22

Abstract

Phosphatase PP2A expression levels are positively correlated to the clinical severity of systemic lupus erythematosus (SLE) and IL17A cytokine overproduction, indicating a potential role of PP2A in controlling T_H17 differentiation and inflammation. By generating a mouse strain with ablation of the catalytic subunit α of PP2A in peripheral mature T cells (PP2A cKO), we demonstrate that the PP2A complex is essential for T_H17 differentiation. These PP2A cKO mice had reduced T_H17 cell numbers and less severe disease in an experimental autoimmune encephalomyelitis (EAE) model. PP2A deficiency also ablated C-terminal phosphorylation of SMAD2 but increased C-terminal phosphorylation of SMAD3. By regulating the activity of RORγt *via* binding, the changes in the phosphorylation status of these R-SMADs reduced *Il17a* gene transcription. Finally, PP2A inhibitors showed similar effects on T_H17 cells as were observed in PP2A cKO mice, i.e., decreased T_H17 differentiation and relative protection of mice from EAE. Taken together, these data demonstrate that phosphatase PP2A is essential for T_H17 differentiation, and that inhibition of PP2A could be a possible therapeutic approach to controlling T_H17-driven autoimmune diseases.

Significance statement

By using a gene knockout that leads to T-cell specific deletion, we reveal the essential role of Ser/Thr phosphatase PP2A in T_H17 differentiation. We also show that this works through the regulation of SMAD2/3 phosphorylation status, which elucidates molecular pathways by which PP2A modulates the expression of T_H17 phenotypes. This finding extends our understanding of the close relationship between PP2A overexpression and inflammatory disease. PP2A is the first Ser/Thr phosphatase shown to be capable of controlling T_H17 differentiation *via* modulating R-SMADs activity. We also demonstrate the translational potential of these findings by showing a therapeutic effect of PP2A inhibitors in controlling autoimmune disease in the EAE model.

Keywords： T_H17，PP2A，TGFβ

/body Introduction.

T-helper type 17 (T_H17) cells, a subset of $CD4^+$ T cells defined by IL17, IL22 and IL21 production, are essential for control and clearance of extracellular bacterial and fungi (1, 2). However, excessive T_H17 responses are involved in chronic inflammation and development of many human autoimmune diseases (3). Upon encountering antigen in the context of a local cytokine milieu including transforming growth factor β (TGFβ) and IL6, naïve $CD4^+$ T cells undergo differentiation into effective T_H17 cells. TGFβ is the principal, essential factor promoting the differentiation of T_H17 cells (4, 5).

Through two related transmembrane Ser/Thr kinase receptors, TGFβ induces Ser/Thr signal cascades in activated T cells. Recent work including work from our lab has revealed the regulatory roles of some other Ser/Thr kinases in this process. For example, both MEKK2/3 and MINK1 suppress T_H17 differentiation through direct phosphorylation of the TGFβ signaling components SMAD2 and SMAD3 (6, 7). Precise regulation of SMAD2/3 Ser/Thr phosphorylation status is thus important in driving T_H17 differentiation (6-8). Dephosphorylation of SMAD2/3 is equally critical in this process but the specific phosphatases that catalyze SMAD2/3 dephosphorylation remain unknown.

As one of the major Ser/Thr phosphatases in eukaryotes, phosphatase PP2A is critical for many cellular functions including cell survival, proliferation, activation and differentiation (9). It has been reported that elevated PP2A expression levels are linked to the upregulation of IL17A production by $CD4^+$ T cells in human systemic lupus erythematosus patients (10). Studies in the PP2Ac transgenic mouse model also demonstrated the relationship and mechanism linking of PP2A and *Il17*-dependent immunopathology (11, 12). PP2A is composed of three polypeptide chains, the structural A, the regulatory B and the catalytic C subunits (13). The heterodimer of the A subunit and the C subunit ($PP2A_A$-$PP2A_C$) forms the PP2A core enzyme that associates with one regulatory B subunit, thus determining the substrate specificity of the holoenzyme complex (13).

In TGFβ signaling, two related regulatory B subunits, Bα (*Ppp2r2a*) and Bδ (*Ppp2r2d*), opposingly modulate TGFβ/Activin/Nodal signaling (14), while carboxy terminal phosphorylation of MAD (the SMAD homolog protein in Drosophila) is negatively regulated by the PP2A inhibitor Okadaic Acid (15). By analogy, these observations suggest that PP2A might be a Ser/Thr phosphorylation modulator involved in controlling T_H17 differentiation.

Here, we present data showing that T_H17 cell polarization was largely impaired when *Ppp2ca* was

77 ablated in mature T cells and rendered resistance towards MOG-induced experimental autoimmune
78 encephalomyelitis (EAE). We also show that PP2A knockout leads to altered activation of R-SMADs
79 (specifically decreasing SMAD2 activation and increasing SMAD3 activation). This synergistically
80 inhibited RORγt mediated *Il17a* transcription. This work thus reveals specific role of PP2A in
81 regulating the canonical TGFβ-R-SMAD-RORγt signaling process during T_H17 differentiation and
82 indicates a possible therapeutic approach for controlling T_H17 driven autoimmune diseases *via*
83 inhibition of PP2A.
84

Results.

Normal T cell development in PP2A cKO mice. To explore the function of PP2A in peripheral T cells, we deleted the dominant PP2A Cα isoform of PP2A catalytic subunit (PP2Ac) in T cell by crossing ^{dis}Lck (dLck) Cre with *Ppp2ca*$^{fl/fl}$ mice (in which exons 3-5 of *Ppp2ca* are *loxP* flanked) (16) to generate *Ppp2ca*$^{fl/fl}$ dLck-Cre (termed PP2A cKO mice) and *Ppp2ca*$^{fl/+}$ dLck-Cre or *Ppp2ca*$^{+/+}$ dLck-Cre mice (collectively called PP2A WT mice here) (*SI Appendix*, Fig. S1A and B). The dLck-Cre was driven by the distal promoter of the lymphocyte protein tyrosine kinase (*Lck*) gene, enabling investigation of the *Ppp2ca* deletion after positive selection in T cells (17).

To assess deletion efficiency, *Ppp2ca* mRNA and protein levels were measured and showed clear reduction in peripheral T cells in PP2A cKO mice, while remaining normal in thymic subsets and splenic B cells (*SI Appendix*, Fig. S1C and D). The catalytic subunit of PP2A has two isoforms, Cα and Cβ (encoded by *Ppp2ca* and *Ppp2cb* respectively). Notably we didn't observe compensatory overexpression of *Ppp2cb* (*SI Appendix*, Fig. S1C). PP2A activity in cKO CD4$^+$ T cells was reduced to half of that measured in WT controls (*SI Appendix*, Fig. S1E).

Analysis of the numbers and frequencies of different T cell subsets in these mice showed that cKO mice exhibited normal T cell development in thymus (*SI Appendix*, Fig. S2A-C) as well as in peripheral lymphoid organs (*SI Appendix*, Fig. S2A, D and E). The proportions of naïve/effective T cells in spleen and mesenteric lymph nodes (MLN) were also similar between WT and cKO littermates (*SI Appendix*, Fig. S2F and G). The normal development of peripheral lymphocytes in PP2A cKO mice allowed further investigation of the role of PP2A in T cell differentiation.

T_H17 cell numbers are reduced in PP2A cKO mice. To clarify whether PP2A is involved in T helper cell lineage commitment, we analyzed the populations of T helper subsets *in vivo*. Interestingly, CD4$^+$ T cells from PP2A cKO mice only contained half the number of T_H17 cells comparing to their WT littermates (*SI Appendix*, Fig. S3A and B), while the numbers of T_H1 and Treg CD4$^+$ T cells were not affected in the peripheral lymphoid organs (*SI Appendix*, Fig. S3A, C, D and F). The frequency of Foxp3$^+$ regulatory T cells in the thymus was also comparable between PP2A WT and cKO mice (*SI Appendix*, Fig. S3E and F). Similarly, subsets analysis of the lamina propria also showed a consistent reduction of T_H17 cells (*SI Appendix*, Fig. S3G and I). These data demonstrate that PP2A is involved in maintaining T_H17 cell composition, while other T cell subsets, including Treg and T_H1, appear unaffected.

PP2A deletion impairs T_H17 differentiation *in vitro*. To investigate whether reduced levels of T_H17 cells in PP2A cKO mice result from impaired T_H17 differentiation, we sorted naïve $CD4^+$ T cells from both WT and cKO cells and polarized them under T_H1, T_H2, T_H17 and iTreg conditions to compare their differentiation efficiencies. The results showed that only the generation of T_H17 cells notably declined with the PP2A deficiency, while other T helper subsets were not affected (Fig. 1*A* and *B* and *SI Appendix*, Fig. S4A and B).The expression levels of *Ppp2ca* mRNA and PP2A Cα protein were more abundant in T_H17 cells than in other T helper subsets (*SI Appendix*, Fig. S4G and H).

p-PP2Ac (Y307) levels, a negative indicator for PP2A activity, are lower in T_H17 and T_H1 than in the other subsets, indicating higher PP2A activity in these two subsets (*SI Appendix*, Fig. S4I). Cytokine production showed similar results, confirming that PP2A deficiency specifically reduced T_H17 differentiation (Fig. 1*C* and *SI Appendix*, Fig. S4C). We further tested the expression of several key T_H17 signature genes and found notably decreased *Il17a* and *Il17f* expression and slightly reduced expression of *Rora* and *Il21*, while the expression of *Rorc*, *Il22* and *Il23r* were not significantly affected (Fig. 1*D*). The alteration of the expression pattern of T_H17 signature genes (including *Il17a* and *Il17f*) induced by PP2A deficiency was also confirmed by an RNAseq analysis (*SI Appendix*, Fig. S5A and B and Dataset 1-3).

The proliferation capacity of WT and cKO T cells was measured under T_H17 conditions and were comparable 2 and 5 days after stimulation (*SI Appendix*, Fig. S4D). Upon PI and Annexin staining, WT and cKO cells showed comparable apoptotic rates (*SI Appendix*, Fig. S4E). Thus, reduced $IL17A^+$ $CD4^+$ T cell levels and IL17A production were not due to either impaired proliferation or increased apoptosis in cKO cells. Furthermore, we did not observe an increased portion of $IFN\gamma^+$ or $Foxp3^+$ $CD4^+$ T cells in cKO T cells under T_H17 conditions, which rules out the likelihood of T_H17 cells converting to other cell subsets in these circumstances (Fig. 1*A* and *SI Appendix*, Fig. S4F). These findings therefore demonstrate a T-cell intrinsic impairment of the T_H17 polarization program upon PP2A deficiency which is independent of proliferation, apoptosis or subset conversion.

Reduced severity of EAE in mice with PP2A deficiency. Given the required role of PP2A in inducing normal T_H17 polarization, the question of whether defective T_H17 PP2A cKO cells also influence T_H17-driven autoimmune disease was investigated *in vivo* using an experimental autoimmune encephalomyelitis (EAE) model. We therefore immunized PP2A WT and cKO mice with myelin

oligodendrocyte glycoprotein peptide of amino acids 35–55 (MOG_{35-55}) to induce EAE.

Clinical scoring showed that PP2A deficiency alleviated symptoms of autoimmunity (Fig. 2*A*). Histological examination showed significantly less mononuclear cell infiltration and demyelination in the cerebral and spinal cord of the cKO mice (Fig. 2*B*). Inflammatory cell infiltration into the central nervous system (CNS) was also greatly diminished in the cKO group (Fig. 2*C*). Although the proportion of $CD4^+$ T cells was unchanged in the CNS of cKO mice, the total numbers of infiltrating $CD4^+$ and $CD8^+$ cells were significantly reduced (Fig. 2*C*). IL17A producing $CD4^+$ T cells were also present in significantly decreased numbers in both the CNS and draining lymph nodes (DLN), whereas the frequencies of IFNγ producing $CD4^+$ T cells were unchanged. (Fig. 2*D-F*). These data indicate that reduced IL17A production upon PP2A cKO results in less severe MOG-induced CNS inflammation. Indeed, *in vitro* MOG recall analysis also showed reduced IL17A production by PP2A cKO splenocytes, while IFNγ production was unaffected (Fig. 2*G*). Intriguingly, $Foxp3^+$ $CD4^+$ T cell proportions were also reduced in the CNS but not in the DLN (Fig. 2*D-F*). This might be explained by markedly milder inflammation in the CNS which consequently recruited less regulatory cells. PP2A cKO mice are thus resistant to EAE and this is strongly correlated with an observed significant reduction in T_H17 cell induction.

Intact TCR and IL6 signaling in PP2A cKO $CD4^+$ T cells. We next investigated how PP2A deficiency affected intracellular signaling in controlling T_H17 cell differentiation. Intact TCR signaling is indispensable for T_H17 commitment (18). However, our results showed that PP2A deficiency did not affect normal CD69 upregulation (*SI Appendix*, Fig. S6A), cell proliferation (*SI Appendix*, Fig. S6B) or production of IL2 or IFNγ (*SI Appendix*, Fig. S6C) following anti-CD3 stimulation. Interestingly, Western Blot analysis showed upregulation of pERK and pP38 in PP2A deficient cells (*SI Appendix*, Fig. S6D) and these two pathways are known to play opposing roles in T_H17 differentiation. Inhibition of MEK-ERK signaling enhances T_H17 differentiation while activation of P38 is critical for optimal T_H17 polarization (19-21). We found that use of an MEK inhibitor (inhibiting ERK, U0126) failed to restore T_H17 differentiation due to PP2A deficiency (*SI Appendix*, Fig. S6E). Thus, subtle changes in MAPKs activation are not correlated with decreased T_H17 differentiation due to PP2A deficiency. PP2A overexpression has been previously reported to upregulate *Il17a* gene transcription by enhancing IRF4 activity (11). However, the observed mRNA, protein and IRF4 activity did not support

involvement of IRF4 in leading to diminished *Il17a* transcription (*SI Appendix*, Fig. S5C-E).

By using the PP2A inhibitor OA, previous work has suggested a possible regulatory role of PP2A in regulating IL6 signaling, including promoting the stability of IL6 receptor gp130 (CD130) (22) and modulating STAT3 phosphorylation (23). However, our experiments did not show any alterations in either IL6 receptor expression (*SI Appendix*, Fig. S7A and B) or STAT3 phosphorylation (Y705 and S727) after IL6 stimulation in cKO T cells (*SI Appendix*, Fig. S7C) thus excluding the possibility that the inhibition of T_H17 differentiation upon PP2A deletion is due to TCR or IL6 signaling changes.

Differential modulation of SMAD2/3 activity by PP2A deficiency restrains T_H17 differentiation. In TGFβ pathway, TGFβ RI and RII, which are reported to be opposingly regulated by two different PP2A B subunits (14), were similarly expressed in PP2A cKO T cells (Fig. 3*A* and *B*). Meanwhile, we found that pSMAD2 (Ser465/467) level was decreased but pSMAD3 (Ser423/425) level was increased after TGFβ stimulation in PP2A cKO cells (Fig. 3*C*). In accordance, SMAD2 hyper-phosphorylation and SMAD3 under-phosphorylation was observed in PP2A Cα overexpressed 293FT cells after TGFβ stimulation (*SI Appendix*, Fig. S8A and B). We next performed the Co-IP assay in Jurkat cells to explore the binding of R-SMADs to PP2Ac. We found that PP2Ac can form stable complex with SMAD2 and SMAD3, which does not depend on either TCR or TGFβ stimulation (*SI Appendix*, Fig. S8C and D).

In addition, *in vitro* dephosphorylation assay showed that PP2A can directly dephosphorylate pSMAD3 (*SI Appendix*, Fig. S8E-G). Studies on SMAD2 and SMAD3 conditional knockout mice have revealed the opposite functions of these two molecules in inducing T_H17 cells (24-27). We thus suspected that the altered activation of SMAD2/3 in PP2A cKO cells might serve as the major contributor towards decreased *Il17a* transcription. Indeed, when we expressed different activation forms of SMAD2/3 (WT, dominant negative form 2SA, constitutive active mutants 2SD) in naïve $CD4^+$ T cells and analyzed cell differentiation in T_H17 condition, the results clearly showed that insufficient activation of SMAD2 caused defective T_H17 differentiation, while constitutively activated SMAD2 promoted optimal T_H17 priming (Fig. 3*D* and *E*). On the contrary, ectopic expression of SMAD3 dramatically repressed T_H17 polarization. Interestingly, a SMAD3-2SA mutant also showed inhibitory activity to T_H17 polarization although to a lesser degree (Fig. 3*F* and *G*), indicating that suppression of T_H17 differentiation by SMAD3 depends on both SMAD3 activation and on its overall expression level. To rule out alterations

in iTreg cell skewing condition in the previous experiments, we also used a series of TGFβ doses for suboptimal iTreg priming but observed no difference between the PP2A cKO and WT groups (*SI Appendix*, Fig. S7D).

Changes in SMAD2/3 activity synergistically downregulate *Il17a* transcription *via* reducing RORγt activity. We next asked how the shift of SMAD2/3 phosphorylation status affected *Il17a* transcription. We found that the protein expression levels of RORγt and RORα were not different in PP2A WT and cKO T_H17 cells (Fig. 4*A* and *B*). More importantly, retrovirus-mediated ectopic expression of RORγt could not completely restore T_H17 potentiation in cKO T cells (Fig. 4*C* and *D*). These data supported the hypothesis that PP2A controlled T_H17 differentiation is independent of RORγt protein expression. To address whether overactivation of SMAD3 and insufficient activation of SMAD2 could work cooperatively to suppress RORγt activity, ChIP analysis of RORγt occupancy of *Il17a* gene region was carried out. The result confirmed our hypothesis that with equal RORγt expression, its activity was largely reduced due to PP2A deficiency (Fig. 4*E*). Phosphorylation changes of SMAD2/3 affected their binding ability with RORγt. In cKO T_H17 cells, RORγt binded more SMAD3 and less SMAD2 than observed in WT T_H17 cells (Fig. 4*F*).

Different activation forms of SMAD2/3 were then co-transfected with RORγt in the 293FT cell line. These experiments showed that the constitutively active SMAD2/3 preferentially interacts with RORγt over the inactive forms, and that SMAD3 is more accessible to bind RORγt than SMAD2 (Fig. 4*G*). These results suggest that phosphorylation changes in SMAD2/3 may inhibit RORγt activity by affecting the capacity of SMAD2/3 to form complexes with RORγt. Based on this hypothesis, we performed rescue experiments with SMAD2-2SD transfection or SMAD3 knockdown. Both approaches significantly improved T_H17 polarization in cKO naïve $CD4^+$ T cells (Fig. 4*H-K*). SMAD3 knockdown efficiency by siRNA was verified by Western Blot and RT-PCR (*SI Appendix*, Fig. S9A and B).

PP2A inhibitors phenocopy phosphorylation changes of SMAD2/3 and restrain T_H17 polarization *in vitro*. We observed that administration of PP2A inhibitors in 293FT cells phenocopied the SMAD2/3 activation changes in a dose dependent manner (Fig. 5*A*). Further, the PP2A inhibitor Cantharidin (CAN) restrained RORγt mediated *Il17a* promoter activation (Fig. 5*B*). More importantly, when administrating PP2A inhibitor Cantharidin in T_H17 culture medium, we also observed a dose dependent

inhibitory role at a concentration that had no effect on cell proliferation (Fig. 5C-E). Another two PP2A inhibitors OA and Fostriecin (FOS) also showed similar effects upon T_H17 differentiation (*SI Appendix*, Fig. S10A-E). In addition, PP2A cKO T cells did not display suppression effects by PP2A inhibitors, ruling out the off-target effects might result in T_H17 depression (Fig. 5*F* and *SI Appendix*, Fig. S10F).

A PP2A inhibitor protects mice from EAE. We examined whether Cantharidin can block T_H17 cell mediated inflammation in EAE. A significant reduction of disease severity was observed in Cantharidin treated PP2A WT mice compared to PBS treated WT mice (Fig. 6*A*). Histological examination also showed significantly less mononuclear cells infiltration and demyelination in the spinal cord of the Cantharidin treated WT mice (Fig. 6*B*). Meanwhile, there was no observable aggravation of clinical symptoms by applying Cantharidin in PP2A cKO mice, suggesting that Cantharidin dose was within a safe range (Fig. 6*A*). Fewer mononuclear lymphocytes and $CD4^+$ T cells infiltrated into the CNS of Cantharidin treated WT mice than of the PBS WT group at the onset or peak of EAE, while the $CD8^+$ and myeloid population was not significantly changed (Fig. 6*C-D*). Additionally, the ratio of T_H17 cells was lower in Cantharidin treated WT mice than in PBS treated WT mice ($p=0.08$) (Fig. 6*E*). The number of infiltrated T_H17 cells was also significantly lower in the CNS. Treg cells and IFNγ producing cells were slightly decreased (Fig. 6*F*). Furthermore, Cantharidin treatment in PP2A cKO groups did not alter the number of inflammatory lymphocytes infiltrated into CNS (Fig. 6*G-H*). Cantharidin treated cKO groups showed no effects to EAE symptoms, suggesting the specific targeting of Cantharidin to PP2A in T cells in this experimental setting. However, whether Cantharidin can also act on other cells and contribute to the therapeutic effects is unclear. Collectively, data above showed that PP2A inhibitor Cantharidin can limit EAE development principally by reducing T_H17 differentiation.

Discussion.

By using peripheral T cell specific KO mice, we have established the positive regulatory role of PP2A in T_H17 differentiation as well as in inflammatory autoimmune diseases. We have also proved that underactivated SMAD2 and overactivated SMAD3 downstream of TGFβ signaling collectively reduced RORγt mediated *Il17a* transcription in PP2A cKO mice. PP2A inhibitors also reduced T_H17 polarization, indicating a promising therapeutic avenue for treating T_H17 cell mediated autoimmune diseases.

PP2A is one of the most abundant phosphatases and crucial for many key cellular events. A total knockout of the PP2A catalytic subunit a in mice is lethal (16). To our surprise, PP2A deficiency did not lead to fundamental changes in basic processes such as cell survival and proliferation. This is either because of the residual PP2A expression in our cKO mice or the stage and cell specific functions of PP2A.

As shown by RNAseq and RT-PCR analysis, the transcriptional changes of T_H17 signature genes induced in PP2A cKO were limited. Obvious changes were observed in *Il17a* and *Il17f*, but not in *Rorc*. Expression of RORγt was intact, which exclude the possibility that PP2A is involved in the pathways leading to RORγt induction. Therefore, intracellular signaling events downstream of RORγt and closely related to *Il17a* transcription might be the candidate targets of PP2A mediated inhibition of T_H17 differentiation.

SMAD2, SMAD3 and SMAD4 are all critical for TGFβ signaling and participate in T_H17 or iTreg cell priming to induce balanced expression of Foxp3 and RORγt (24-26, 28-30). It is intriguing that SMAD2 knockout mice show reduced T_H17 cell differentiation and ameliorated EAE, while a deficiency in SMAD3 has the opposite effects (24, 26-28). Furthermore, overexpression of SMAD2 and RORγt augments the differentiation of T_H17 cells. However, SMAD3 binds to RORγt in Co-IP experiments and decreases its transcriptional activity (26). Moreover, R-SMAD activation is mainly *via* the phosphorylation of the C-terminal SSXS motif, which is critical for R-SMAD function. The active form of SMAD3 might enhance its binding affinity with RORγt and it is known that SMAD3 can compete with SMAD2 for binding with RORγt (27). These results suggest that active SMAD2 plays a positive role and active SMAD3 plays a negative role in T_H17 cell differentiation likely *via* dynamic interaction with RORγt (26, 27).

Our study confirmed that altered SMAD2/3 activation by PP2A affects T_H17 differentiation, resulting

in decreased *Il17a* transcription *via* forming complex with RORγt and reducing its activity and thus affecting T_H17 differentiation. Importantly, this is the first study to identify PP2A as the critical phosphatase responsible for Ser/The dephosphorylation on R-SMADs and necessary for efficient T_H17 differentiation.

It is important to know the precise dephosphorylation site on R-SMAD and the responsible kinases. Our previous work has elucidated the importance of threonine residue T324 in the α-helix 1 region of SMAD2 for regulation during T_H17 differentiation (6). It is thus likely that PP2A upregulates SMAD2 C-terminal phosphorylation *via* modulating MINK1 activity. However, the function of PP2A appears to be broader and more dominant than this single phosphorylation event, since we also observed increased SMAD3 phosphorylation in cKO $CD4^+$ T cells, which also contributes to deceased T_H17 differentiation. This observation is in accordance with a previous finding that the PP2A structural subunit PR65 could interact with SMAD3 (31).

It is also likely that PP2A directly regulates the phosphorylation status of RORγt. Recent study showed that two functional phosphorylation sites identified on RORγt played opposite roles in T_H17 polarization. IKKα was discovered as upper stream regulator for the phosphorylation change (32). Whether PP2A participates in the interaction with IKKα or RORγt in regulating RORγt activity remains to be elucidated.

The classical TGFβ pathway is also critical for iTreg differentiation (33). SMAD2 and SMAD3 double knockout mice showed dramatic loss of Foxp3 induction (28). Then why is iTreg differentiation not affected by PP2A deficiency? It is most likely because of the redundant roles of SMAD2 and SMAD3 in TGFβ induced iTreg plasticity (28). Overactivated SMAD3 may compensate for insufficient activation of SMAD2 in Foxp3 induction. In a recent study, PP2A was reported to be indispensable for the maintenance of the suppressive function of Treg cells via regulating the activity of the mTORC1 complex. Specific ablation of PP2A in Treg cells by Foxp3-YFP-Cre leads to autoimmunity with similar clinical features of scurfy mice (34). We also observed the same Treg phenotype in dLck-driven PP2A cKO mice, but the overall outcome of PP2A defect in peripheral T cells is dominated by T_H17 differentiation impairment, which is demonstrated by their reduced susceptibility to autoimmune diseases induction.

Finally, in addition of finding the importance of PP2A to T_H17 differentiation, we demonstrated the

translational potential of this pathway by showing the therapeutic effect of PP2A inhibitor in controlling autoimmune diseases in the EAE model.

Materials and Methods.

Mice. *Ppp2ca* flowed mice were provided by X. Gao, Model Animal Research Center of Nanjing University. Mice with Cre recombinase driven by the distal promoter of the gene encoding the kinase Lck were bought from the Jackson Laboratory. The experimental protocols were approved by the Review Committee of Zhejiang University School of Medicine and followed institutional guidelines.

EAE Induction. EAE was induced as described previously (35). Briefly, mice aged 6-8 weeks were immunized with 200 mg MOG_{35-55} (Sangon, MEVGWYRSPFSRVVHLYRNGK) in an equal amount of Complete Freund's Adjuvant (Chondrex, Inc.) and received 200 ng pertussis toxin (List Biochemicals) intravenously on days 0 and 2 post-induction. Clinical evaluation was assigned daily using a 5-point scale: 1, flaccid tail; 2, impaired righting reflex and hindlimb weakness; 3, hindlimb paralysis; 4, hindlimb and forelimb paralysis; 5, moribund. Detailed materials and methods are presented fully in SI Appendix, SI Materials and Methods.

Statistical Analysis. Statistical analysis was performed using GraphPad Prism. The data were analyzed by Student's t-test. All P value less than 0.05 was considered significant ($P < 0.05$ = *; $P < 0.01$ = **; $P < 0.001$ = ***).

ACKONWLEDGMENTS. The authors thank Dr. Dawang Zhou for providing plasmids in Luciferase Assay and Dr. Xinhua Feng for providing ALK5(202D)-HA plasmid. We are grateful to Youfa Zhu, Yanwei Li, Jiajia Wang, and Yingying Huang from the core facilities (Zhejiang University School of Medicine) for technical assistance in histology and FACS analysis. This work was supported by grants from the National Natural Science Foundation of China (31770954 and 31530019 to L.L., 81570013 to S.W, and 31500708 to M.Z.), National Key R&D Program of China (2018YFC1105102 to L.L.) and Fundamental Research Funds for the Central Universities (2018XZZX001-12 to L.L.).

ACCESSION NUMBER: RNAseq data is under GEO database GSE119836.

AUTHOR CONTRIBUTIONS. Q.X., M.Z., S.W., R.S., H.H., X.G. and L.L. designed the research; Q.X., X.J., M.Z., D.R., G.F. and Z.W. performed the research; Q.X., X.J. and L.L. analyzed the data; Q.X., X.J., R.S., L.W., H.H. and L.L. wrote the paper.

Reference

1. Bai H, Gao X, Zhao L, Peng Y, Yang J, Qiao S, Zhao H, Wang S, Fan Y, & Joyee AG (2017) Respective IL-17A production by γδ T and Th17 cells and its implication in host defense against chlamydial lung infection. *Cellular & molecular immunology* **14**(10):850.

2. Simonian PL, Roark CL, Wehrmann F, Lanham AM, Born WK, O'Brien RL, & Fontenot AP (2009) IL-17A-expressing T cells are essential for bacterial clearance in a murine model of hypersensitivity pneumonitis. *The Journal of Immunology* **182**(10):6540-6549.

3. Wong CK, Lit LCW, Tam LS, Li EKM, Wong PTY, & Lam CWK (2008) Hyperproduction of IL-23 and IL-17 in patients with systemic lupus erythematosus: implications for Th17-mediated inflammation in auto-immunity. *Clinical immunology* **127**(3):385-393.

4. Mangan PR, Harrington LE, O'quinn DB, Helms WS, Bullard DC, Elson CO, Hatton RD, Wahl SM, Schoeb TR, & Weaver CT (2006) Transforming growth factor-β induces development of the TH17 lineage. *Nature* **441**(7090):231-234.

5. Veldhoen M, Hocking RJ, Atkins CJ, Locksley RM, & Stockinger B (2006) TGFβ in the context of an inflammatory cytokine milieu supports de novo differentiation of IL-17-producing T cells. *Immunity* **24**(2):179-189.

6. Fu G, Xu Q, Qiu Y, Jin X, Xu T, Dong S, Wang J, Ke Y, Hu H, & Cao X (2017) Suppression of Th17 cell differentiation by misshapen/NIK-related kinase MINK1. *Journal of Experimental Medicine*:jem. 20161120.

7. Chang X, Liu F, Wang X, Lin A, Zhao H, & Su B (2011) The kinases MEKK2 and MEKK3 regulate transforming growth factor-β-mediated helper T cell differentiation. *Immunity* **34**(2):201-212.

8. Derynck R & Zhang YE (2003) Smad-dependent and Smad-independent pathways in TGF-β family signalling. *Nature* **425**(6958):577-584.

9. Seshacharyulu P, Pandey P, Datta K, & Batra SK (2013) Phosphatase: PP2A structural importance, regulation and its aberrant expression in cancer. *Cancer letters* **335**(1):9-18.

10. Katsiari CG, Kyttaris VC, Juang Y-T, & Tsokos GC (2005) Protein phosphatase 2A is a negative regulator of IL-2 production in patients with systemic lupus erythematosus. *The Journal of clinical investigation* **115**(11):3193-3204.

11. Apostolidis SA, Rauen T, Hedrich CM, Tsokos GC, & Crispín JC (2013) Protein phosphatase 2A enables expression of interleukin 17 (IL-17) through chromatin remodeling. *Journal of Biological Chemistry* **288**(37):26775-26784.

12. Crispín JC, Apostolidis SA, Rosetti F, Keszei M, Wang N, Terhorst C, Mayadas TN, & Tsokos GC (2012) Cutting edge: protein phosphatase 2A confers susceptibility to autoimmune disease through an IL-17–dependent mechanism. *The Journal of Immunology*:1200143.

13. Cho US & Xu W (2007) Crystal structure of a protein phosphatase 2A heterotrimeric holoenzyme. *Nature* **445**(7123):53-57.

14. Batut J, Schmierer B, Cao J, Raftery LA, Hill CS, & Howell M (2008) Two highly related regulatory subunits of PP2A exert opposite effects on TGF-β/Activin/Nodal

385 signalling. *Development* **135**(17):2927-2937.

386 15. Kaneko S, Chen X, Lu P, Yao X, Wright TG, Rajurkar M, Kariya K-i, Mao J, Ip YT, &
387 Xu L (2011) Smad inhibition by the Ste20 kinase Misshapen. *Proceedings of the*
388 *National Academy of Sciences* **108**(27):11127-11132.

389 16. Gu P, Qi X, Zhou Y, Wang Y, & Gao X (2012) Generation of Ppp2Ca and Ppp2Cb
390 conditional null alleles in mouse. *genesis* **50**(5):429-436.

391 17. Zhang DJ, Wang Q, Wei J, Baimukanova G, Buchholz F, Stewart AF, Mao X, & Killeen
392 N (2005) Selective expression of the Cre recombinase in late-stage thymocytes using
393 the distal promoter of the Lck gene. *The Journal of Immunology* **174**(11):6725-6731.

394 18. Molinero LL, Cubre A, Mora-Solano C, Wang Y, & Alegre M-L (2012) T cell
395 receptor/CARMA1/NF-κB signaling controls T-helper (Th) 17 differentiation.
396 *Proceedings of the National Academy of Sciences* **109**(45):18529-18534.

397 19. Tan AH-M & Lam K-P (2010) Pharmacologic inhibition of MEK–ERK signaling
398 enhances Th17 differentiation. *The journal of immunology* **184**(4):1849-1857.

399 20. Noubade R, Krementsov DN, Del Rio R, Thornton T, Nagaleekar V, Saligrama N,
400 Spitzack A, Spach K, Sabio G, & Davis RJ (2011) Activation of p38 MAPK in CD4 T
401 cells controls IL-17 production and autoimmune encephalomyelitis. *Blood*
402 **118**(12):3290-3300.

403 21. Di Mitri D, Sambucci M, Loiarro M, De Bardi M, Volpe E, Cencioni MT, Gasperini C,
404 Centonze D, Sette C, & Akbar AN (2015) The p38 mitogen-activated protein kinase
405 cascade modulates T helper type 17 differentiation and functionality in multiple
406 sclerosis. *Immunology* **146**(2):251-263.

22. Mitsuhashi S, Shima H, Tanuma N, Sasa S, Onoe K, Ubukata M, & Kikuchi K (2005) Protein phosphatase type 2A, PP2A, is involved in degradation of gp130. *Molecular and cellular biochemistry* **269**(1):183-187.

23. Woetmann A, Nielsen M, Christensen ST, Brockdorff J, Kaltoft K, Engel A-M, Skov S, Brender C, Geisler C, & Svejgaard A (1999) Inhibition of protein phosphatase 2A induces serine/threonine phosphorylation, subcellular redistribution, and functional inhibition of STAT3. *Proceedings of the National Academy of Sciences* **96**(19):10620-10625.

24. Yoon J-H, Sudo K, Kuroda M, Kato M, Lee I-K, Han JS, Nakae S, Imamura T, Kim J, & Ju JH (2015) Phosphorylation status determines the opposing functions of Smad2/Smad3 as STAT3 cofactors in TH17 differentiation. *Nature communications* **6**.

25. Malhotra N, Robertson E, & Kang J (2010) SMAD2 is essential for TGFβ-mediated Th17 cell generation. *Journal of Biological Chemistry* **285**(38):29044-29048.

26. Martinez GJ, Zhang Z, Chung Y, Reynolds JM, Lin X, Jetten AM, Feng X-H, & Dong C (2009) Smad3 differentially regulates the induction of regulatory and inflammatory T cell differentiation. *Journal of Biological Chemistry* **284**(51):35283-35286.

27. Martinez GJ, Zhang Z, Reynolds JM, Tanaka S, Chung Y, Liu T, Robertson E, Lin X, Feng X-H, & Dong C (2010) Smad2 positively regulates the generation of Th17 cells. *Journal of Biological Chemistry* **285**(38):29039-29043.

28. Takimoto T, Wakabayashi Y, Sekiya T, Inoue N, Morita R, Ichiyama K, Takahashi R, Asakawa M, Muto G, & Mori T (2010) Smad2 and Smad3 Are Redundantly Essential for the TGF-β–Mediated Regulation of Regulatory T Plasticity and Th1 Development.

The Journal of Immunology **185**(2):842-855.

29. Tone Y, Furuuchi K, Kojima Y, Tykocinski ML, Greene MI, & Tone M (2008) Smad3 and NFAT cooperate to induce Foxp3 expression through its enhancer. *Nature immunology* **9**(2):194.

30. Zhang S, Takaku M, Zou L, Chou W-c, Zhang G, Wu B, Kong Q, Thomas SY, Serody JS, & Chen X (2017) Reversing SKI–SMAD4-mediated suppression is essential for T H 17 cell differentiation. *Nature* **551**(7678):105.

31. Heikkinen PT, Nummela M, Leivonen S-K, Westermarck J, Hill CS, Kähäri V-M, & Jaakkola PM (2010) Hypoxia-activated Smad3-specific dephosphorylation by PP2A. *Journal of Biological Chemistry* **285**(6):3740-3749.

32. He Z, Wang F, Zhang J, Sen S, Pang Q, Luo S, Gwack Y, & Sun Z (2017) Regulation of Th17 Differentiation by IKKα-Dependent and-Independent Phosphorylation of RORγt. *The Journal of Immunology* **199**(3):955-964.

33. Zhou L, Lopes JE, Chong MM, Ivanov II, Min R, Victora GD, Shen Y, Du J, Rubtsov YP, & Rudensky AY (2008) TGF-β-induced Foxp3 inhibits TH17 cell differentiation by antagonizing RORγt function. *Nature* **453**(7192):236-240.

34. Apostolidis SA, Rodríguez-Rodríguez N, Suárez-Fueyo A, Dioufa N, Ozcan E, Crispín JC, Tsokos MG, & Tsokos GC (2016) Phosphatase PP2A is requisite for the function of regulatory T cells. *Nature immunology* **17**(5):556-564.

35. Yao Y, Han W, Liang J, Ji J, Wang J, Cantor H, & Lu L (2013) Glatiramer acetate ameliorates inflammatory bowel disease in mice through the induction of Qa-1-restricted CD8+ regulatory cells. *European journal of immunology* **43**(1):125-136.

Figure legends

Fig 1. PP2A deficiency specifically limits T_H17 differentiation *in vitro*.

(A, B) Flow cytometry (A) and quantification (B) of IL17A staining in naïve $CD4^+$ T cells from PP2A WT and cKO mice differentiated under T_H17 polarizing condition for 5 days. (C) Enzyme-linked immunosorbent assay (ELISA) of IL17A in the culture medium of each polarizing condition (n=3 technical replicates). (D) RT-PCR analysis of T_H17 signature genes (n=3 technical replicates). Each symbol represents an individual mouse (n=8), error bars show mean ± SEM. Data are representative of at least three independent experiments with similar results.

Fig 2. Loss of PP2A protects mice from EAE by repressing IL17A production.

(A) Mean clinical scores for EAE from each group. (B) Representative histology of the brain and spinal cord (hematoxylin and eosin (H&E) on the left and luxol fast blue (LFB) on the right) of mice after EAE induction (day 19). Arrowheads indicate inflammatory infiltration (left) and demyelination (right). Scale bars represent 100 μm. (C) Number and frequency of mononuclear cells or $CD4^+$ or $CD8^+$ T cells infiltrated into central nervous system. (D) Flow cytometry of IL17A, IFNγ and Foxp3 staining from CNS (left panel) or DLN (right panel) $CD4^+$ T cells. (E, F) Quantification of $IL17A^+$, $IFN\gamma^+$ and $Foxp3^+$ $CD4^+$ T cells in CNS (E) or DLN (F). (G) Splenocytes were rechallenged with MOG peptide (5μg/ml) or control vehicle for 3 days, and cytokine production was measured by ELISA. Each symbol represents an individual mouse (n=4-6); error bars show mean ± SEM. Data are representative of three independent experiments with similar results.

Fig 3. Insufficient SMAD2 activation and overactivated SMAD3 under TGFβ pathway restrains T_H17 differentiation.

(A, B) Histograms (A) and mean fluorescence intensity (MFI) quantification (B) of TGFβ receptor I and II staining on CD4 gated cells from splenocytes of PP2A WT and cKO mice. (C) Enriched $CD4^+$ T cells from PP2A WT and cKO were stimulated with 10 ng/ml TGFβ as indicated, whole cell lysates were probed with the indicated antibodies in the immunoblots. (D, E) Flow cytometry (D) and quantification (E) of T_H17 polarization with ectopic expression of Vector, WT, 2SA and 2SD of SMAD2 in WT naïve $CD4^+$ T cells. GFP expressing cells were gated for analysis on day 3. (F, G) Flow cytometry (F) and quantification (G) of T_H17 polarization with ectopic expression of Vector, WT, 2SA and 2SD of SMAD3 in WT naïve $CD4^+$ T cells. GFP expressing cells were gated for analysis on day 3. Each symbol represents an individual mouse (n=4). Error bars show mean ± SEM. Data are representative of three independent experiments (C) or two independent experiments with two replicates (D, F).

Fig 4. Differential modulation of SMAD2/3 inhibits RORγt mediated *Il17a* transcription by forming complex with RORγt.

(A) Flow cytometry of RORγt staining from naïve $CD4^+$ T cells primed under T_H17 polarizing condition for 2 days. (B) RORα was immunoblotted with whole cell lysate of T_H17 cells. (C-D) Flow cytometry (C) and quantification (D) of T_H17 polarization with ectopic expression of Vector or RORγt

in PP2A WT and cKO naïve $CD4^+$ T cells. GFP expressing cells were gated for analysis on day 3. (E) RORγt binding to the sites of the *Il17a* gene promoter was analyzed by using chromatin immunoprecipitation (ChIP) assay with RT-PCR. (F) Co-IP analysis of binding ability with RORγt among SMAD2/3 in WT and cKO T_H17 cells. (G) Co-IP analysis of binding ability with RORγt among WT, 2SA and 2SD mutant of SMAD2/3 in 293FT cells. (H) Flow cytometry of T_H17 polarization with ectopic expression of Vector or SMAD2-2SD in PP2A WT and cKO naïve $CD4^+$ T cells. (I) Ratio of IL17A frequency comparing VEC-cKO or SMAD2-2SD-cKO to VEC-WT. (J) Flow cytometry of T_H17 polarization after suppressing SMAD3 expression by siRNA in naïve $CD4^+$ T cells. (K) The ratio of IL17A frequency in cKO cells transfected with siRNA-SMAD3 or control to the frequency of WT cells transfected with control. Error bars show mean ± SEM. Data are representative of three (A, B, G, H, J) or two (C, D, E, F) independent experiments.

Fig 5. PP2A inhibitors lead the same change of SMAD2/3 activation under TGFβ pathway and limit T_H17 priming *in vitro*.

(A) SMAD2/3 was overexpressed in the 293FT cells and PP2A inhibitors were added in serum free medium for 2 hours followed by TGFβ (3 ng/ml) stimulation for 3 hours. Western Blot analysis using phospho-specific SMAD2/3 (p-SMAD2/3) and FLAG-tag (total-SMAD2/3) antibodies. (B) *Il17a* promoter and SMAD2/3 with or without RORγt was transfected into 293FT cells and then treated with PP2A inhibitors and TGFβ as Figure (A). Luciferase activity was measured and normalized based on Renilla luciferase gene. (C) Sorted naïve $CD4^+$ T cells were polarized under T_H17 priming condition with the indicated concentration of Cantharidin for 3 days and $IL17A^+$ population was analyzed using flow cytometry on day 5. (D) The concentration of IL17A in the culture supernatant was measured by ELISA. (E) Histogram of CFSE fluorescence staining of cells in Figure (C). (F) WT naïve $CD4^+$ T cells cultured with Cantharidin (5μM) for the first 3 days in T_H17 priming condition and analyzed $IL17A^+$ population by flow cytometry on day 5. Error bars show mean ± SEM. Data are representative of two independent experiments with similar results.

Fig 6. A PP2A inhibitor suppresses EAE development.

(A) PP2A WT and cKO mice were immunized with $MOG_{(35-55)}$ peptide. PP2A inhibitor Cantharidin (0.6 μg/g) was administered intraperitoneally daily from day 10 to day 12 and then was given once every two days. Mean clinical scores for EAE from each group. (B) Representative histology of the spinal cord (H&E left and LFB right) of mice after EAE induction (day 19). Arrowheads indicate inflammatory infiltration (left) and demyelination (right). Scale bars represent 100 μm. (C) Quantification of total mononuclear cells, $CD4^+$ T cells, $CD8^+$ T cells and myeloid cells that infiltrated into the CNS of WT mice at peak of the disease. (D) Ratio of $CD4^+$ and $CD8^+$ T cells (gated at $CD45^{hi}$ $CD11b^-$) in the CNS of WT groups. (E, F) Ratio (E) and number (F) of $IL17A^+$ or $Foxp3^+$ or $IFNγ^+$ $CD4^+$ cells in the CNS of the WT groups at disease peak. (G) Quantification of total mononuclear cells, $CD4^+$ T cells, $CD8^+$ T cells and myeloid cells that infiltrated into the CNS of the cKO groups. (H) Ratio of $CD4^+$ and $CD8^+$ T cells (gated at $CD45^{hi}$ $CD11b^-$) that infiltrated into the CNS of the cKO groups. Each symbol represents an individual mouse (n=5-7 per genotype); error bars show mean ± SEM. Data are representative of two independent experiments with similar results.

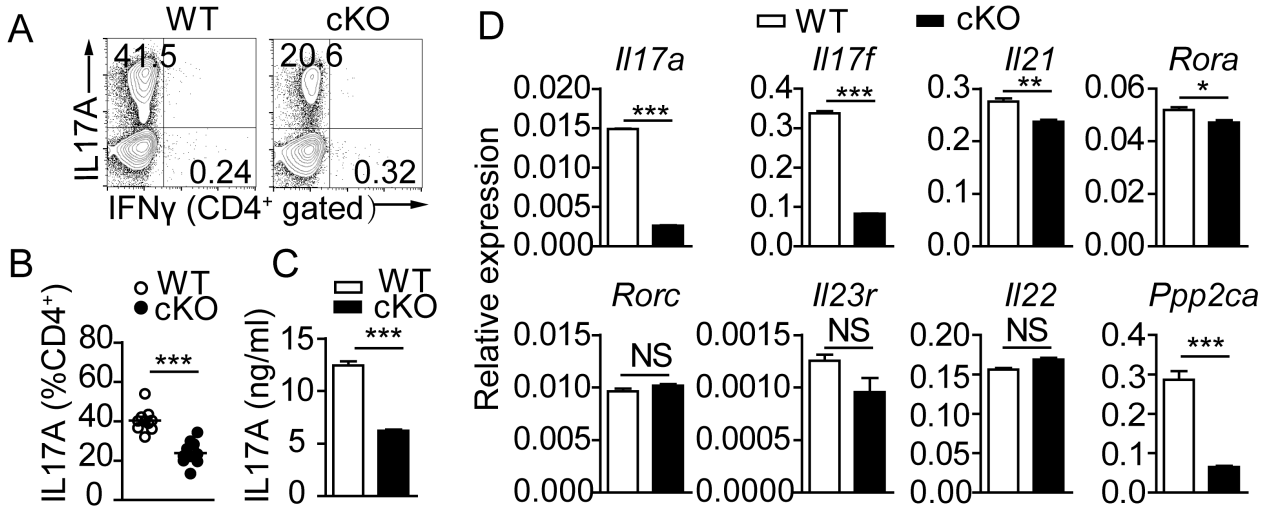
A
WT
cKO
41.5
0.24
20.6
0.32
IL17A
IFNγ (CD4+ gated)
B
WT
cKO
IL17A (%CD4+)
80
60
40
20
0
***
C
WT
cKO
IL17A (ng/ml)
15
10
5
0
***
D
WT
cKO
Relative expression
Il17a
***
0.020
0.015
0.010
0.005
0.000
Il17f
***
0.4
0.3
0.2
0.1
0.0
Il21
**
0.3
0.2
0.1
0.0
Rora
*
0.06
0.04
0.02
0.00
Rorc
NS
0.015
0.010
0.005
0.000
Il23r
NS
0.0015
0.0010
0.0005
0.0000
Il22
NS
0.20
0.15
0.10
0.05
0.00
Ppp2ca
***
0.4
0.3
0.2
0.1
0.0

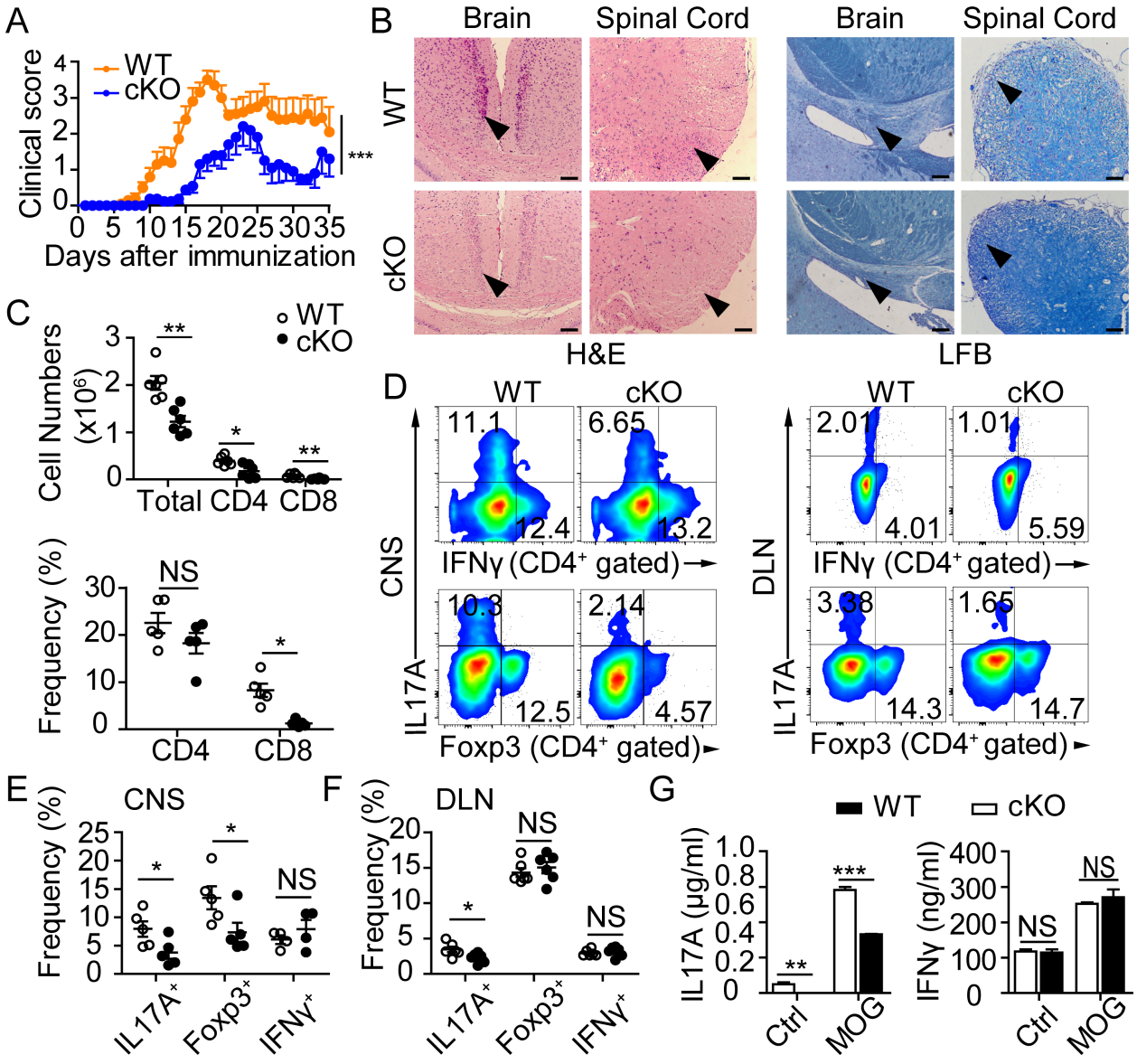
A
Clinical score
WT
cKO
***
Days after immunization
B
Brain
Spinal Cord
Brain
Spinal Cord
WT
cKO
H&E
LFB
C
Cell Numbers (x10^6)
WT
cKO
Total
CD4
CD8
Frequency (%)
NS
CD4
CD8
D
WT
cKO
CNS
IFNγ (CD4+ gated)
IL17A
Foxp3 (CD4+ gated)
11.1
6.65
12.4
13.2
10.3
2.14
12.5
4.57
DLN
2.01
1.01
4.01
5.59
3.38
1.65
14.3
14.7
E
CNS
Frequency (%)
IL17A+
Foxp3+
IFNγ+
F
DLN
G
WT
cKO
IL17A (μg/ml)
IFNγ (ng/ml)
Ctrl
MOG

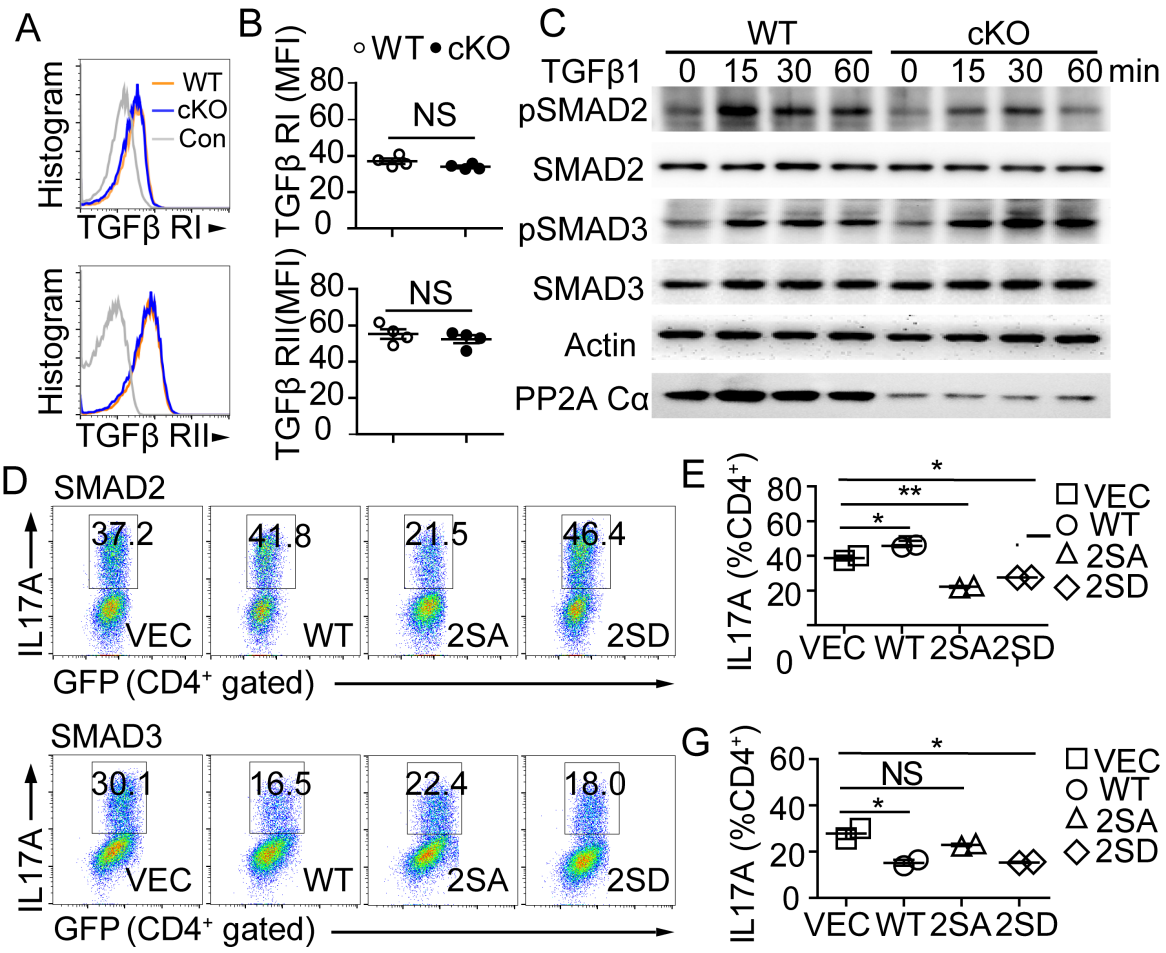
A
Histogram
WT
cKO
Con
TGFβ RI
Histogram
TGFβ RII
B
WT cKO
TGFβ RI (MFI)
NS
TGFβ RII(MFI)
NS
C
WT
cKO
TGFβ1
0 15 30 60 0 15 30 60 min
pSMAD2
SMAD2
pSMAD3
SMAD3
Actin
PP2A Cα
D
SMAD2
37.2
41.8
21.5
46.4
VEC
WT
2SA
2SD
IL17A
GFP (CD4+ gated)
SMAD3
30.1
16.5
22.4
18.0
E
IL17A (%CD4+)
VEC
WT
2SA
2SD
G
NS

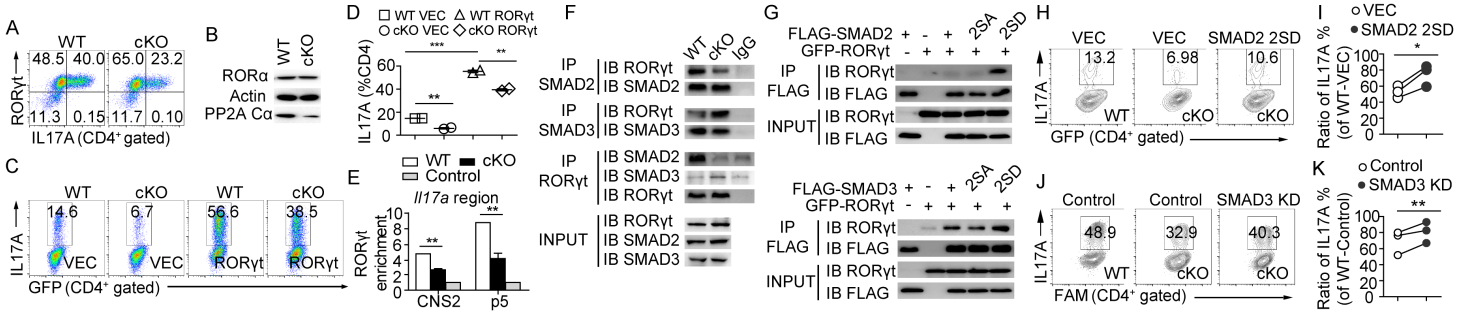
A
WT
cKO
48.5
40.0
65.0
23.2
11.3
0.15
11.7
0.10
RORγt
IL17A (CD4+ gated)
B
WT
cKO
RORα
Actin
PP2A Cα
C
WT
cKO
WT
cKO
14.6
6.7
56.6
38.5
VEC
VEC
RORγt
RORγt
IL17A
GFP (CD4+ gated)
D
WT VEC
WT RORγt
cKO VEC
cKO RORγt
IL17A (%CD4)
E
WT
cKO
Control
Il17a region
RORγt enrichment
CNS2
p5
F
WT
cKO
IgG
IP SMAD2
IB RORγt
IB SMAD2
IP SMAD3
IB RORγt
IB SMAD3
IP RORγt
IB SMAD2
IB SMAD3
IB RORγt
INPUT
IB RORγt
IB SMAD2
IB SMAD3
G
FLAG-SMAD2
GFP-RORγt
2SA
2SD
IP FLAG
IB RORγt
IB FLAG
INPUT
IB RORγt
IB FLAG
FLAG-SMAD3
GFP-RORγt
2SA
2SD
IP FLAG
IB RORγt
IB FLAG
INPUT
IB RORγt
IB FLAG
H
VEC
VEC
SMAD2 2SD
13.2
6.98
10.6
WT
cKO
cKO
IL17A
GFP (CD4+ gated)
J
Control
Control
SMAD3 KD
48.9
32.9
40.3
WT
cKO
cKO
IL17A
FAM (CD4+ gated)
I
VEC
SMAD2 2SD
Ratio of IL17A % (of WT-VEC)
K
Control
SMAD3 KD
Ratio of IL17A % (of WT-Control)

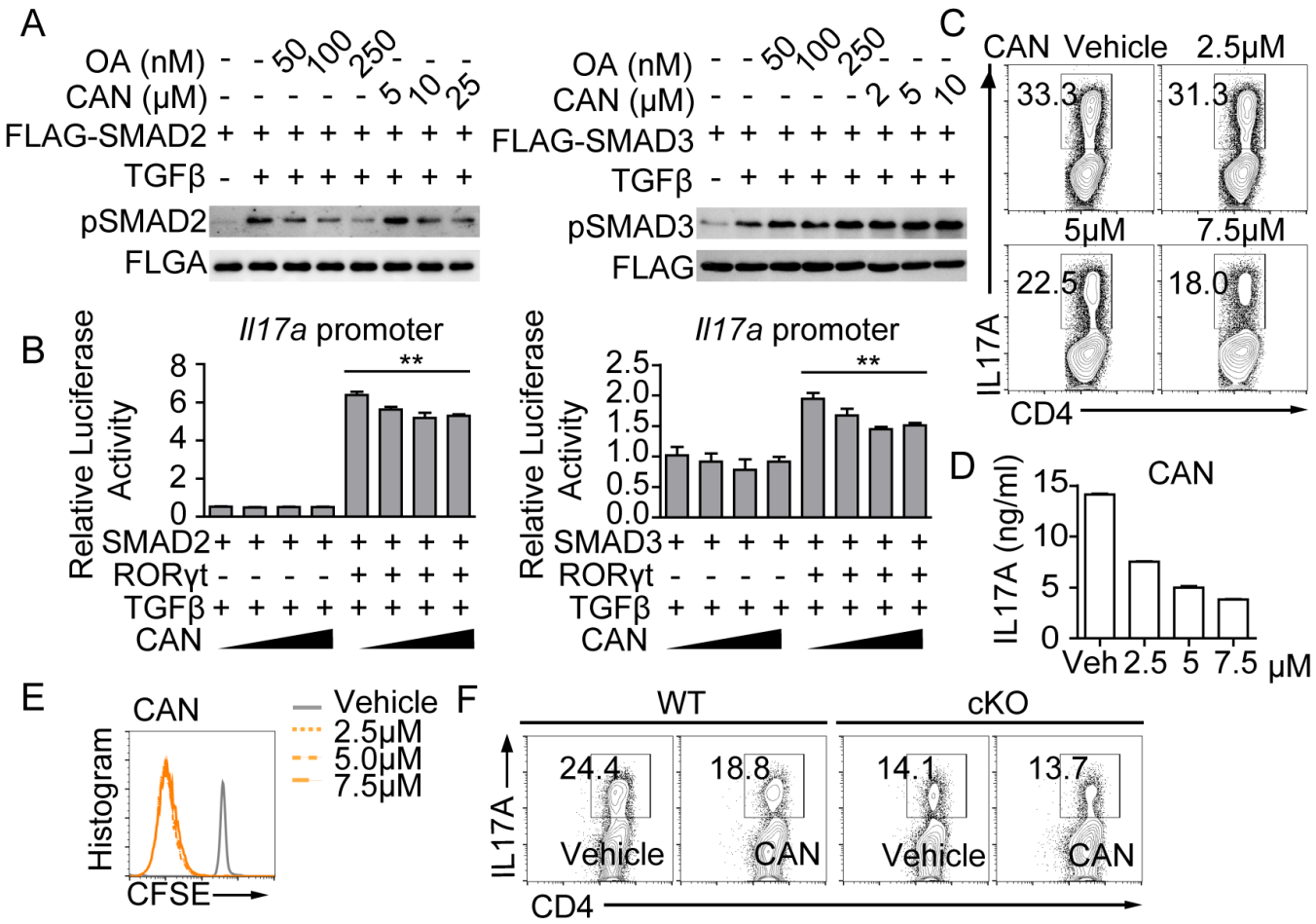
A
OA (nM) - - 50 100 250 - - -
CAN (μM) - - - - - 5 10 25
FLAG-SMAD2 + + + + + + + +
TGFβ - + + + + + + +
pSMAD2
FLGA
OA (nM) - - 50 100 250 - - -
CAN (μM) - - - - - 2 5 10
FLAG-SMAD3 + + + + + + + +
TGFβ - + + + + + + +
pSMAD3
FLAG
B
Il17a promoter
Relative Luciferase Activity
**
SMAD2 + + + + + + + +
RORγt - - - - + + + +
TGFβ + + + + + + + +
CAN
Il17a promoter
Relative Luciferase Activity
**
SMAD3 + + + + + + + +
RORγt - - - - + + + +
TGFβ + + + + + + + +
CAN
C
CAN Vehicle 2.5μM 5μM 7.5μM
33.3
31.3
22.5
18.0
IL17A
CD4
D
CAN
IL17A (ng/ml)
Veh 2.5 5 7.5 μM
E
CAN
Vehicle
2.5μM
5.0μM
7.5μM
Histogram
CFSE
F
WT
cKO
24.4
18.8
14.1
13.7
Vehicle
CAN
Vehicle
CAN
IL17A
CD4

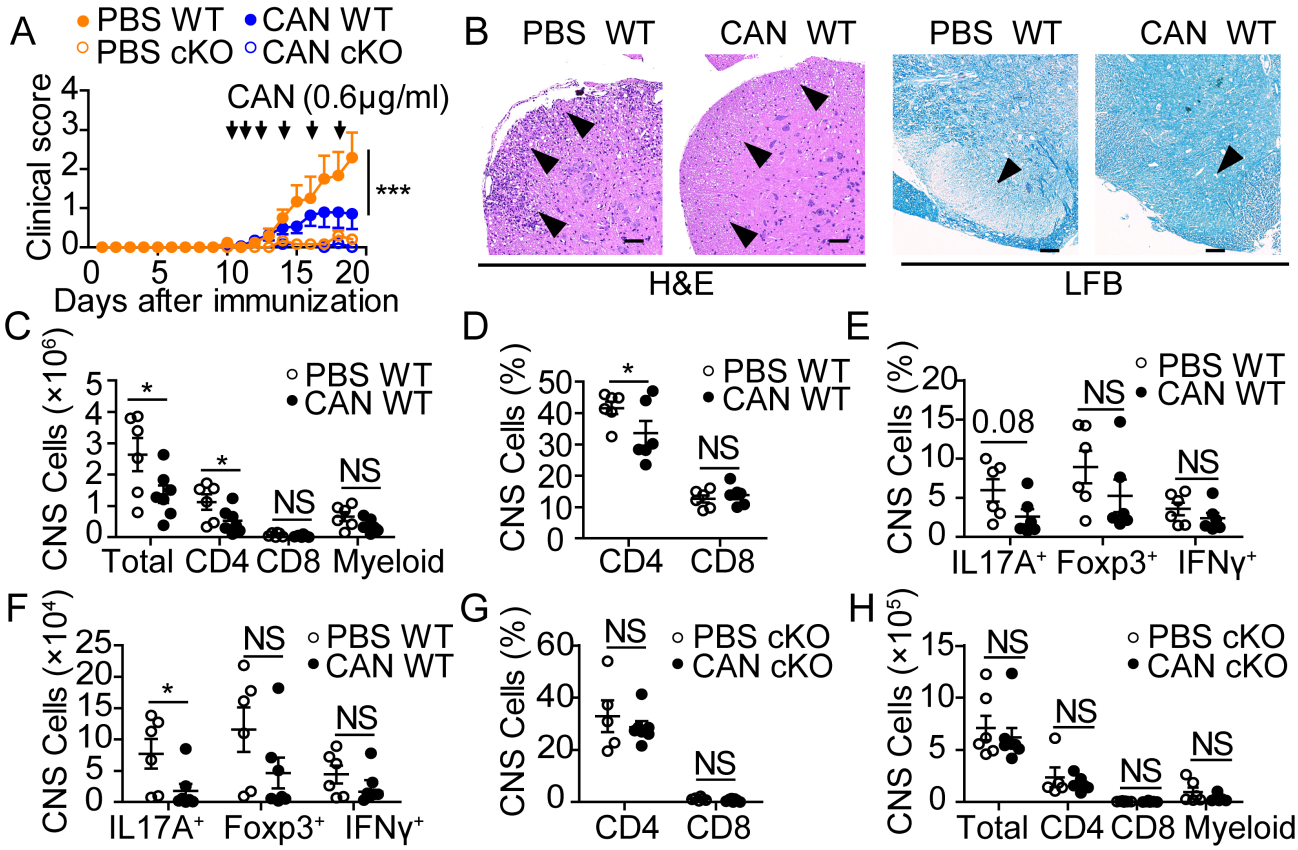
A
PBS WT
CAN WT
PBS cKO
CAN cKO
CAN (0.6μg/ml)
Clinical score
Days after immunization
***
B
PBS WT
CAN WT
H&E
LFB
C
CNS Cells (×10⁶)
Total
CD4
CD8
Myeloid
D
CNS Cells (%)
E
0.08
IL17A⁺
Foxp3⁺
IFNγ⁺
F
CNS Cells (×10⁴)
G
PBS cKO
CAN cKO
H
CNS Cells (×10⁵)
NS